

# SCIENTIFIC REPORTS



OPEN

## The $\beta$ and $\gamma$ subunits play distinct functional roles in the $\alpha_2\beta\gamma$ heterotetramer of human NAD-dependent isocitrate dehydrogenase

Received: 18 October 2016  
Accepted: 28 December 2016  
Published: 31 January 2017

Tengfei Ma<sup>1</sup>, Yingjie Peng<sup>1</sup>, Wei Huang<sup>1</sup>, Yabing Liu<sup>2</sup> & Jianping Ding<sup>1,3,4,5</sup>

Human NAD-dependent isocitrate dehydrogenase existing as the  $\alpha_2\beta\gamma$  heterotetramer, catalyzes the decarboxylation of isocitrate into  $\alpha$ -ketoglutarate in the Krebs cycle, and is allosterically regulated by citrate, ADP and ATP. To explore the functional roles of the regulatory  $\beta$  and  $\gamma$  subunits, we systematically characterized the enzymatic properties of the holoenzyme and the composing  $\alpha\beta$  and  $\alpha\gamma$  heterodimers in the absence and presence of regulators. The biochemical and mutagenesis data show that  $\alpha\beta$  and  $\alpha\gamma$  alone have considerable basal activity but the full activity of  $\alpha_2\beta\gamma$  requires the assembly and cooperative function of both heterodimers.  $\alpha_2\beta\gamma$  and  $\alpha\gamma$  can be activated by citrate or/and ADP, whereas  $\alpha\beta$  cannot. The binding of citrate or/and ADP decreases the  $S_{0.5, \text{isocitrate}}$  and thus enhances the catalytic efficiencies of the enzymes, and the two activators can act independently or synergistically. Moreover, ATP can activate  $\alpha_2\beta\gamma$  and  $\alpha\gamma$  at low concentration and inhibit the enzymes at high concentration, but has only inhibitory effect on  $\alpha\beta$ . Furthermore, the allosteric activation of  $\alpha_2\beta\gamma$  is through the  $\gamma$  subunit not the  $\beta$  subunit. These results demonstrate that the  $\gamma$  subunit plays regulatory role to activate the holoenzyme, and the  $\beta$  subunit the structural role to facilitate the assembly of the holoenzyme.

Mitochondrial NAD-dependent isocitrate dehydrogenases (NAD-IDHs, EC 1.1.1.41) in eukaryotes are a family of enzymes that catalyze the oxidative decarboxylation of isocitrate (ICT) into  $\alpha$ -ketoglutarate ( $\alpha$ -KG) while reducing NAD to NADH in the rate-limiting step of the Krebs cycle. Those enzymes are conserved from yeast to mammals and consist of multiple subunits<sup>1</sup>. They are all allosteric enzymes under strict cellular regulation, which can be activated by AMP (in yeast) or ADP (in mammals) and citrate (CIT) but inhibited by ATP (in mammals) and NADH. Thus, the cellular ratios of [ATP]/[AMP or ADP] and [NADH]/[NAD] can regulate the activity of NAD-IDH in the Krebs cycle and influence the energy production and substance flux in cells.

Mammalian NAD-IDHs isolated from porcine heart<sup>2–8</sup>, porcine liver<sup>9</sup>, bovine heart<sup>10–12</sup>, and ox brain<sup>13</sup> have been biochemically characterized. All these enzymes are consisted of three types of subunits in the ratio of  $2\alpha:1\beta:1\gamma$ , and exist as the  $\alpha_2\beta\gamma$  heterotetramer composed of the  $\alpha\beta$  and  $\alpha\gamma$  heterodimers, which can be further dimerized into a heterooctamer (the heterotetramer and heterooctamer are sometimes called holoenzyme and hereafter we will not distinguish the heterotetramer, heterooctamer and holoenzyme in the biochemical context unless otherwise specified). The  $\alpha$ ,  $\beta$  and  $\gamma$  subunits have molecular masses of 37 kDa, 39 kDa and 39 kDa, respectively, and exhibit distinct isoelectric points. The  $\alpha$  and  $\beta$  subunits share about 40% sequence identity, the  $\alpha$  and

<sup>1</sup>National Center for Protein Science Shanghai, State Key Laboratory of Molecular Biology, Center for Excellence in Molecular Cell Science, Institute of Biochemistry and Cell Biology, Shanghai Institutes for Biological Sciences, Chinese Academy of Sciences, 320 Yueyang Road, Shanghai 200031, China. <sup>2</sup>School of Life Sciences, Shanghai University, 333 Nanchen Road, Shanghai 200444, China. <sup>3</sup>School of Life Science and Technology, ShanghaiTech University, 100 Haik Road, Shanghai 201210, China. <sup>4</sup>Shanghai Science Research Center, Chinese Academy of Sciences, 333 Haik Road, Shanghai 201210, China. <sup>5</sup>Collaborative Innovation Center for Genetics and Development, Fudan University, 2005 Songhu Road, Shanghai 200438, China. Correspondence and requests for materials should be addressed to J.D. (email: jpding@sibcb.ac.cn)

$\gamma$  subunits about 42% sequence identity, and the  $\beta$  and  $\gamma$  subunits about 52% sequence identity<sup>14,15</sup>. The previous biochemical studies showed that the individual  $\alpha$ ,  $\beta$  or  $\gamma$  subunit of porcine heart NAD-IDH isolated using urea (2M) is either inactive or exhibits very low activity, but the recombined  $\alpha$  and  $\beta$  subunits or  $\alpha$  and  $\gamma$  subunits in the form of the  $\alpha\beta$  or  $\alpha\gamma$  heterodimer shows considerable activity<sup>2</sup>. All mammalian NAD-IDHs require divalent metal ions such as  $Mn^{2+}$ ,  $Mg^{2+}$ ,  $Co^{2+}$ , and  $Cd^{2+}$  for the activity<sup>16–19</sup>. In addition, the activity could be positively regulated by CIT and ADP but inhibited by ATP and NADH<sup>7,11,20</sup>. It was suggested that these enzymes have two binding sites per heterotetramer for each ligand, including ICT,  $Mn^{2+}$ , NAD, and ADP<sup>4,21</sup>.

Recombinant human NAD-IDH was successfully expressed in *E. coli*, which allowed more mutagenesis and biochemical studies of the enzyme based on sequence alignment with *E. coli* and porcine mitochondrial NADP-IDHs<sup>19,22–25</sup>. Those studies examined the functional roles of several strictly conserved residues of the  $\alpha$ ,  $\beta$  and  $\gamma$  subunits in the bindings of metal ion, ICT, NAD, and ADP, and showed that the  $\alpha$  subunit is critical for the catalytic activity, and the  $\beta$  and  $\gamma$  subunits play functional roles in allosteric regulation; however, the  $\alpha$  subunit alone has no detectable activity and its coexistence with one of the two regulatory subunits is essential for the activity.

*Saccharomyces cerevisiae* NAD-IDH exists as a heterotetramer composed of two heterodimers of the regulatory subunit IDH1 and catalytic subunit IDH2, which can be further assembled into a heterooctamer. The structures of yeast NAD-IDH in apo form, in CIT bound form, and in CIT-AMP bound form have been determined at moderate resolution<sup>26</sup>, which revealed the assembly of the heterotetramer and heterooctamer and the binding sites of the activators. IDH1 and IDH2 form a compact heterodimer that acts as the basic functional and structural unit, and the structural communication between the two subunits is considered to be important to the allosteric regulation.

As human NAD-IDH contains three types of subunits, the molecular mechanism of allosteric regulation appears to be more complex than that of yeast NAD-IDH. In addition, the enzymatic properties of the composing  $\alpha\beta$  and  $\alpha\gamma$  heterodimers and the exact functional roles of the  $\beta$  and  $\gamma$  subunits in the  $\alpha_2\beta\gamma$  heterotetramer are not well understood. Thus, human NAD-IDH is a very good model for studying the molecular mechanism of allosteric regulation. Moreover, mutations of human NADP-dependent IDHs localized in the cytoplasm and mitochondria (also called IDH1 and IDH2) have been identified in multiple types of tumors and the mutant proteins confer neomorphic activity to convert  $\alpha$ -KG into 2-hydroxyglutarate (2-HG) whose accumulation can result in epigenetic dysregulation, leading to oncogenesis and development of tumors<sup>27–32</sup>. Intriguingly, human NAD-IDH (also called IDH3) has also recently been implicated in some diseases. Homozygous mutations of the  $\beta$  subunit are suggested to be a cause of retinitis pigmentosa, a hereditary degeneration of the retina leading to blindness<sup>33</sup>. Aberrant expression of the  $\alpha$  subunit can promote malignant tumor growth by inducing HIF-1-mediated metabolic reprogramming and angiogenesis<sup>34</sup>. Abnormalities of human NAD-IDH are associated with pathogenesis of major psychiatric disorders<sup>35</sup>. Furthermore, human NAD-IDH is shown to be a novel target of tributyltin, an environmental contaminant chemical, in human embryonic carcinoma cells<sup>36</sup>. Thus, the structural and mechanistic studies of human NAD-IDH have also important biomedical implications.

In this work, we systematically studied the enzymatic properties the  $\alpha\beta$  and  $\alpha\gamma$  heterodimers and the  $\alpha_2\beta\gamma$  heterotetramer of human NAD-IDH in the absence and presence of several regulators including CIT, ADP and ATP. Our biochemical data show that the  $\alpha\gamma$  heterodimer has similar enzymatic properties and kinetic parameters as the  $\alpha_2\beta\gamma$  heterotetramer, whereas the  $\alpha\beta$  heterodimer has only basal activity and cannot be allosterically regulated. The catalytic efficiencies of the  $\alpha_2\beta\gamma$  and  $\alpha\gamma$  enzymes are activated by CIT or/and ADP through decreasing the  $S_{0.5}$  for ICT. Additionally, the two activators can function synergistically, suggesting that CIT and ADP can bind to the enzymes independently and cooperatively. Moreover, ATP can activate the  $\alpha_2\beta\gamma$  and  $\alpha\gamma$  enzymes at low concentration in a manner similar to ADP and inhibit the activities at high concentration, but has only inhibitory effect on the  $\alpha\beta$  enzyme. Furthermore, the mutagenesis data show that the  $\alpha\beta$  and  $\alpha\gamma$  heterodimers contribute equally to the activity of the  $\alpha_2\beta\gamma$  heterotetramer in either the absence or presence of the activators, and the allosteric regulation of the  $\alpha_2\beta\gamma$  heterotetramer is through the  $\gamma$  subunit not the  $\beta$  subunit. These results together demonstrate that the  $\gamma$  subunit plays the regulatory role to activate the holoenzyme, and the  $\beta$  subunit the structural role to facilitate the assembly of the holoenzyme. These findings provide new insights into the molecular mechanisms of the function and allosteric regulation of mammalian NAD-IDHs.

## Results

**Preparation of human NAD-IDH.** The  $\alpha\beta$  and  $\alpha\gamma$  heterodimers and the  $\alpha_2\beta\gamma$  heterotetramer of human NAD-IDH were prepared as described in “Methods”. *In vitro* assembly of the  $\alpha_2\beta\gamma$  heterotetramer from the  $\alpha\beta$  and  $\alpha\gamma$  heterodimers gave a much higher yield than the co-expression method, and the  $\alpha_2\beta\gamma$  heterotetramer obtained using both methods exhibited no difference in enzymatic properties, and thus we used the assembled  $\alpha_2\beta\gamma$  heterotetramer in all the biochemical studies. SDS-PAGE analyses showed that the purified  $\alpha_2\beta\gamma$  protein and  $\alpha\beta$  and  $\alpha\gamma$  proteins are of sufficient purity (>95%) and there are two protein bands with equal intensity that are characteristic of mammalian NAD-IDHs<sup>5,25,37</sup>, with the upper band corresponding to the  $\beta$  or/and  $\gamma$  subunits (39 kDa) and the lower band corresponding to the  $\alpha$  subunit (37 kDa) (Fig. 1a). Size-exclusion chromatography coupled with multi-angle light scattering (SEC-MALS) analyses showed that the  $\alpha_2\beta\gamma$  protein exhibits an elution volume of about 11 ml with an average molecular mass of about 288 kDa corresponding to a dimer of heterotetramer or a heterooctamer (theoretical molecular mass of 304 kDa), which is in agreement with the previous reports for the recombinant human NAD-IDH<sup>24,25</sup> and the isolated pig heart NAD-IDH<sup>3</sup>. Both the  $\alpha\beta$  and  $\alpha\gamma$  proteins exhibit an elution volume of about 14 ml at the injection protein concentration of 2 mg/ml with an average molecular mass of about 79 kDa corresponding to the  $\alpha\beta$  and  $\alpha\gamma$  heterodimers (theoretical molecular mass of 76 kDa), but exhibit an elution volume of about 13 ml at the injection protein concentration of 12 mg/ml with an average molecular mass of about 130 kDa corresponding to dimers of heterodimers (theoretical molecular mass of 152 kDa) (Fig. 1b). These results indicate that the  $\alpha_2\beta\gamma$  protein exists as a heterooctamer in solution; the  $\alpha\beta$

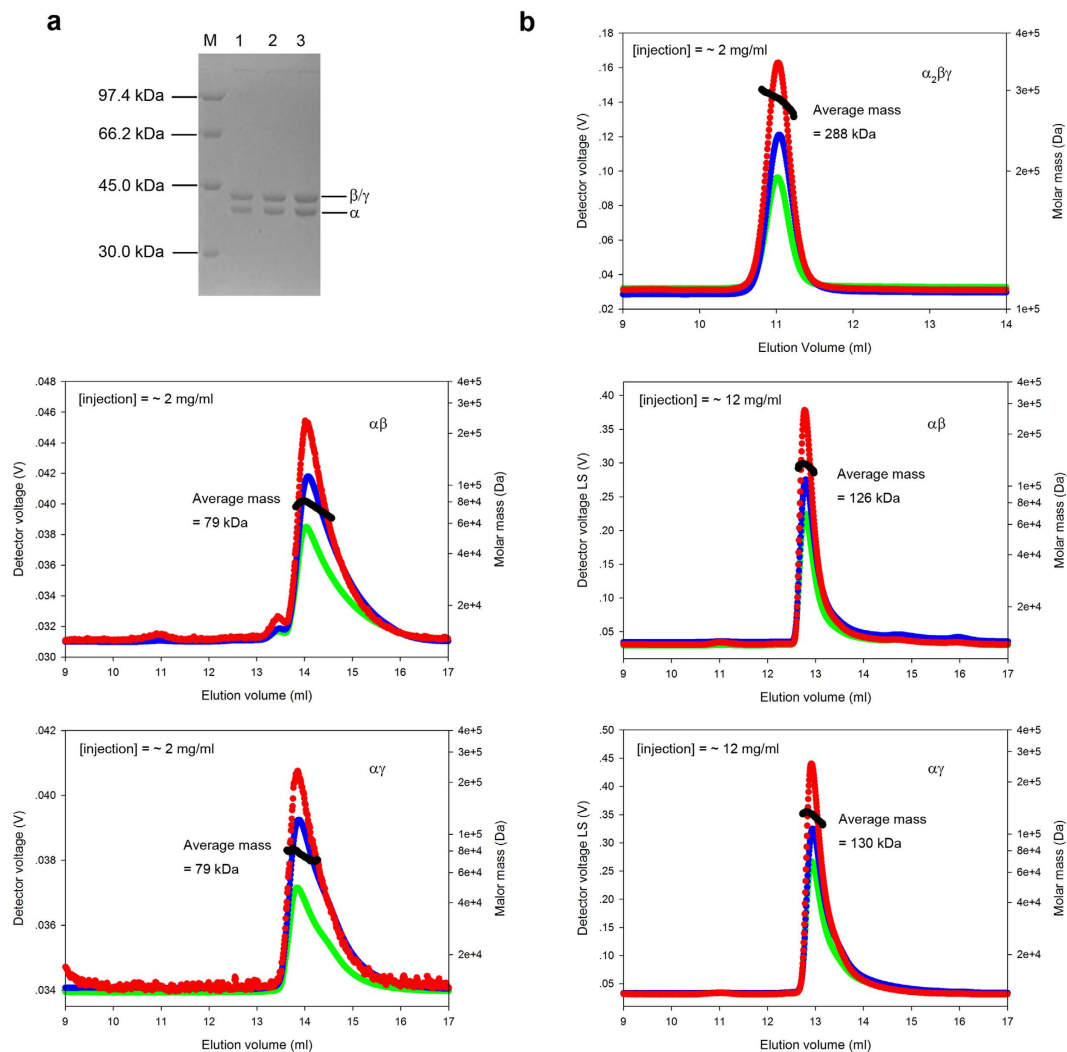


**Figure 1.** SDS-PAGE and SEC-MALS analyses of the  $\alpha_2\beta\gamma$  heterotetramer and the  $\alpha\beta$  and  $\alpha\gamma$  heterodimers of human NAD-IDH. (a) SDS-PAGE (12%) analyses of the  $\alpha_2\beta\gamma$  heterotetramer and the  $\alpha\beta$  and  $\alpha\gamma$  heterodimers with Coomassie blue staining. M, molecular mass standards; lane 1, the  $\alpha_2\beta\gamma$  heterotetramer; lane 2, the  $\alpha\beta$  heterodimer; lane 3, the  $\alpha\gamma$  heterodimer. The upper band represents the  $\beta$  or/and  $\gamma$  subunits (39 kDa), and the lower band represents the  $\alpha$  subunit (37 kDa). The ratio of the catalytic subunit and regulatory subunit(s) in all three samples is 1:1. (b) SEC-MALS analyses of the  $\alpha_2\beta\gamma$ ,  $\alpha\beta$  and  $\alpha\gamma$  proteins. Chromatograms show the readings from the light scattering (red) at  $90^\circ$ , refractive index (blue), and UV (green) detectors. The left and right vertical axes represent the light scattering detector reading and the molecular mass. The black curve represents the calculated molecular mass. The  $\alpha\beta$  and  $\alpha\gamma$  proteins show an elution peak at about 14 ml corresponding to an average molecular mass of about 79 kDa at the injection protein concentration of 2 mg/ml, and an elution peak at about 13 ml corresponding to an average molecular mass of about 130 kDa at the injection protein concentration of 12 mg/ml. The  $\alpha_2\beta\gamma$  protein shows an elution peak at about 11 ml corresponding to an average molecular mass of about 288 kDa at the injection protein concentration of 2 mg/ml.

and  $\alpha\gamma$  proteins exist as heterodimers at low concentration but as dimers of heterodimers at high concentration. As the final protein concentrations in the enzymatic studies were below  $0.2 \mu\text{g/ml}$ , presumably the  $\alpha\beta$  and  $\alpha\gamma$  proteins exist mainly as heterodimers and the  $\alpha_2\beta\gamma$  protein as a heterooctamer.

**Enzymatic properties of human NAD-IDH.** The  $\alpha_2\beta\gamma$  protein has a specific activity of  $20.2 \pm 0.3 \mu\text{mol/min/mg}$  at the standard conditions, and the  $\alpha\beta$  and  $\alpha\gamma$  proteins exhibit specific activities of  $3.33 \pm 0.13 \mu\text{mol/min/mg}$  and  $7.27 \pm 0.31 \mu\text{mol/min/mg}$  (about 16.5% and 36.0% of that of the  $\alpha_2\beta\gamma$  protein), respectively, which are comparable to those of the isolated pig heart NAD-IDH<sup>2</sup> and the purified  $\alpha_2\beta\gamma$  enzyme of human NAD-IDH<sup>19</sup>, but are significantly higher than those of the unpurified human NAD-IDH<sup>22</sup> (Table 1). These results indicate that both the  $\alpha\beta$  and  $\alpha\gamma$  heterodimers have considerable basal activities with the  $\alpha\gamma$  heterodimer having about 2-fold higher activity than the  $\alpha\beta$  heterodimer, and the full activity of the  $\alpha_2\beta\gamma$  heterotetramer requires the assembly and cooperative functions of both heterodimers.

Enzyme	Specific activity ( $\mu\text{mol}/\text{min}/\text{mg}$ )			
	This work	Ehrlich <i>et al.</i> <sup>2</sup>	Soundar <i>et al.</i> <sup>19</sup>	Kim <i>et al.</i> <sup>22</sup>
$\alpha_2\beta\gamma$	20.2 $\pm$ 0.3	15–20	21.7	0.2359 $\pm$ 0.0320
$\alpha\beta$	3.33 $\pm$ 0.13	2.9		0.0046 $\pm$ 0.0002
$\alpha\gamma$	7.27 $\pm$ 0.31	7.8		0.0255 $\pm$ 0.0007

**Table 1. Specific activities of the  $\alpha_2\beta\gamma$ ,  $\alpha\beta$  and  $\alpha\gamma$  enzymes.** The specific activities of the enzymes were measured at the standard conditions: 33 mM Tris-acetate, pH 7.4, 80 mM ICT, 2 mM  $\text{MnCl}_2$ , and 3.2 mM NAD.

Enzyme	$V_{\text{max,ICT}}$	$S_{0.5,ICT}$	Hill coefficient for ICT	$S_{0.5,\text{Mn}}$	$S_{0.5,\text{NAD}}$	$k_{\text{cat}}^a$	$k_{\text{cat}}/S_{0.5,ICT}$
	$\mu\text{mol}/\text{mg}/\text{min}$	mM		$\mu\text{M}$	$\mu\text{M}$	$\text{s}^{-1}$	$\text{s}^{-1}\text{mM}^{-1}$
$\alpha_2\beta\gamma$	20.0 $\pm$ 0.1	2.35 $\pm$ 0.05	2.0 $\pm$ 0.1	60.2 $\pm$ 6.0	143 $\pm$ 5	26.7 $\pm$ 0.1	11.36 $\pm$ 0.04
$\alpha\beta$	10.9 $\pm$ 0.3	13.4 $\pm$ 0.1	1.1 $\pm$ 0.0	5305 $\pm$ 314	326 $\pm$ 15	14.6 $\pm$ 0.4	1.08 $\pm$ 0.03
$\alpha\gamma$	7.29 $\pm$ 0.11	4.49 $\pm$ 0.15	2.0 $\pm$ 0.1	95.1 $\pm$ 3.2	238 $\pm$ 18	9.72 $\pm$ 0.15	2.16 $\pm$ 0.03

**Table 2. Kinetic parameters of the  $\alpha_2\beta\gamma$ ,  $\alpha\beta$  and  $\alpha\gamma$  enzymes in the absence of any regulators.** The  $V_{\text{max}}$  and  $S_{0.5}$  of the  $\alpha_2\beta\gamma$  and  $\alpha\gamma$  enzymes were determined at the standard conditions with varied concentrations of ICT, or  $\text{MnCl}_2$ , or NAD. The  $V_{\text{max}}$  and  $S_{0.5}$  of the  $\alpha\beta$  enzyme were determined at the same conditions but with higher concentration of  $\text{MnCl}_2$  (50 mM). <sup>a</sup>A molecular mass of 80 kDa was used to calculate the mole of enzyme in heterodimeric form per mg of protein ( $1.25 \times 10^{-8}$  mol of dimeric enzyme/mg of protein).

The previous biochemical data showed that mammalian NAD-IDHs require divalent metal ions for their activities<sup>2,19</sup>. Consistently, our biochemical data show that the  $\alpha_2\beta\gamma$ ,  $\alpha\beta$  and  $\alpha\gamma$  enzymes all require divalent metal ions for their activities but have different  $S_{0.5}$  values. The  $\alpha_2\beta\gamma$  enzyme has a  $S_{0.5}$  value of  $60.2 \pm 6.0 \mu\text{M}$  for  $\text{Mn}^{2+}$ , the  $\alpha\gamma$  enzyme has a slightly higher  $S_{0.5}$  (1.6-fold), but the  $\alpha\beta$  enzyme has a significantly higher  $S_{0.5}$  (88-fold) (Table 2). We also analyzed the effects of different metal ions on the activities of these enzymes, and among the six metal ions tested ( $\text{Mn}^{2+}$ ,  $\text{Mg}^{2+}$ ,  $\text{Co}^{2+}$ ,  $\text{Zn}^{2+}$ ,  $\text{Ni}^{2+}$  and  $\text{Ca}^{2+}$ ),  $\text{Mn}^{2+}$  is the most effective one (Supplementary Table S1). Thus, we used  $\text{Mn}^{2+}$  in all the activity assays and kinetic studies.

**Activation of human NAD-IDH by CIT or/and ADP.** The previous biochemical data showed that the activities of mammalian NAD-IDHs can be positively regulated by CIT and ADP<sup>1,11,20</sup>. To investigate the activation effects of CIT or/and ADP on the  $\alpha_2\beta\gamma$ ,  $\alpha\beta$  and  $\alpha\gamma$  enzymes, we first measured their kinetic parameters in the absence of any regulators. Our results show that the  $\alpha_2\beta\gamma$  enzyme has a  $V_{\text{max,ICT}}$  of  $20.0 \pm 0.1 \mu\text{mol}/\text{min}/\text{mg}$ , and  $S_{0.5,ICT}$ ,  $S_{0.5,\text{Mn}}$  and  $S_{0.5,\text{NAD}}$  of  $2.35 \pm 0.05$  mM,  $60.2 \pm 6.0 \mu\text{M}$ , and  $143 \pm 5 \mu\text{M}$ , respectively (Table 2). The  $\alpha\gamma$  enzyme has a  $V_{\text{max,ICT}}$  of  $7.29 \pm 0.11 \mu\text{mol}/\text{min}/\text{mg}$  and  $S_{0.5,ICT}$ ,  $S_{0.5,\text{Mn}}$  and  $S_{0.5,\text{NAD}}$  of  $4.49 \pm 0.15$  mM,  $95.1 \pm 3.2 \mu\text{M}$ , and  $238 \pm 18 \mu\text{M}$ , respectively, which are comparable to those of the  $\alpha_2\beta\gamma$  enzyme. As a result, the basal catalytic efficiency ( $k_{\text{cat}}/S_{0.5,ICT}$ ) of the  $\alpha\gamma$  enzyme is about 19.0% of that of the  $\alpha_2\beta\gamma$  enzyme. As the  $\alpha\beta$  enzyme has a very high  $S_{0.5,\text{Mn}}$  and its kinetic parameters could not be obtained at the standard conditions, we measured its kinetic parameters at a substantially increased concentration of  $\text{MnCl}_2$  (50 mM vs. 2 mM). At this condition, the  $\alpha\beta$  enzyme has a slightly lower  $V_{\text{max,ICT}}$  ( $10.9 \pm 0.3 \mu\text{mol}/\text{min}/\text{mg}$ ) but moderately to substantially higher  $S_{0.5,ICT}$  ( $13.4 \pm 0.1$  mM, 5.7-fold),  $S_{0.5,\text{Mn}}$  ( $5305 \pm 314 \mu\text{M}$ , 88-fold) and  $S_{0.5,\text{NAD}}$  ( $326 \pm 15 \mu\text{M}$ , 2.3-fold) than the  $\alpha_2\beta\gamma$  enzyme, and the basal catalytic efficiency is about 9.5% of that of the  $\alpha_2\beta\gamma$  enzyme (Table 2). These data indicate that in the absence of any regulators, the  $\alpha\gamma$  enzyme exhibits similar kinetic properties and has comparable kinetic parameters as the  $\alpha_2\beta\gamma$  enzyme, but the  $\alpha\beta$  enzyme does not.

We then measured the kinetic parameters of the  $\alpha_2\beta\gamma$ ,  $\alpha\beta$  and  $\alpha\gamma$  enzymes in the presence of activator(s) (Fig. 2 and Table 3). Compared with those in the absence of any regulators, in the presence of CIT, ADP and both activators, the  $V_{\text{max,ICT}}$  of the  $\alpha_2\beta\gamma$  enzyme has no significant change but the  $S_{0.5,ICT}$  is decreased by 1.9, 2.7 and 14.6 folds, respectively; and similarly, the  $V_{\text{max,ICT}}$  of the  $\alpha\gamma$  enzyme is slightly increased by 1.2–1.8 folds but the  $S_{0.5,ICT}$  is decreased by 1.7, 2.7 and 24.7 folds, respectively. In contrast, addition of CIT or/and ADP has no significant effects on the  $V_{\text{max,ICT}}$  and  $S_{0.5,ICT}$  of the  $\alpha\beta$  enzyme. As a result, the catalytic efficiencies of the  $\alpha_2\beta\gamma$  and  $\alpha\gamma$  enzymes are substantially increased by about 15.3 and 44.8 folds, respectively; whereas that of the  $\alpha\beta$  enzyme is not affected. Thus, the catalytic efficiency of the  $\alpha\gamma$  enzyme is elevated to about 55.6% of that of the  $\alpha_2\beta\gamma$  enzyme, while that of the  $\alpha\beta$  enzyme is only about 0.7% of that of the  $\alpha_2\beta\gamma$  enzyme (Table 3). These data indicate that the binding of CIT or/and ADP to the  $\alpha_2\beta\gamma$  and  $\alpha\gamma$  enzymes potentiates their activities mainly through decreasing the  $S_{0.5,ICT}$  without significantly affecting the  $V_{\text{max}}$  and the  $k_{\text{cat}}$ . As either CIT or ADP can slightly decrease the  $S_{0.5,ICT}$  of the  $\alpha_2\beta\gamma$  and  $\alpha\gamma$  enzymes but the two activators together can substantially decrease the  $S_{0.5,ICT}$  (Table 3), these data suggest that the two activators can bind either independently or simultaneously to distinct sites at the allosteric site, and the two activators function in a synergistic manner. These results are consistent with the previous biochemical data showing that ADP can positively regulate the activity of mammalian NAD-IDH<sup>7</sup>, and the binding of ADP and CIT can lower the  $S_{0.5,ICT}$  but has no effect on the  $V_{\text{max}}$ <sup>20,38</sup>. These data further demonstrate that in the presence of CIT or/and ADP, the  $\alpha\gamma$  enzyme also exhibits similar kinetic properties as the  $\alpha_2\beta\gamma$  enzyme, but the  $\alpha\beta$  enzyme does not.

Moreover, our kinetic data show that in the absence of any regulators, both the  $\alpha_2\beta\gamma$  and  $\alpha\gamma$  enzymes exhibit a Hill coefficient of 2 with respect to ICT, whereas the  $\alpha\beta$  enzyme exhibits a Hill coefficient of 1, indicating that the

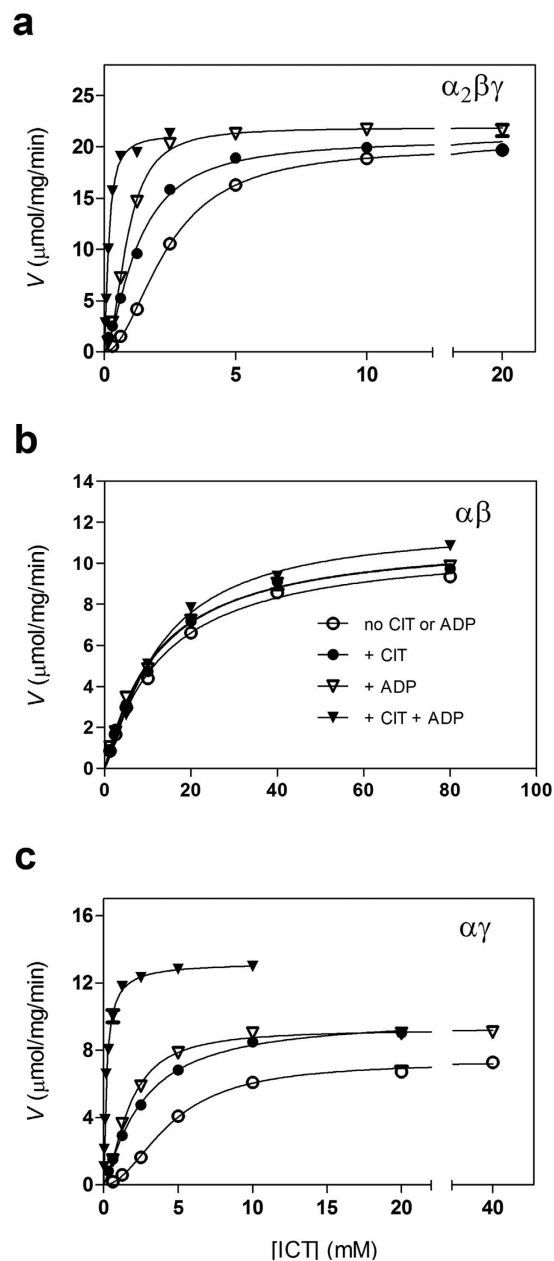


**Figure 2.** Saturation curves of the  $\alpha_2\beta\gamma$  heterotetramer and the  $\alpha\beta$  and  $\alpha\gamma$  heterodimers for isocitrate in the absence and presence of positive regulator(s). (a) Saturation curves of the  $\alpha_2\beta\gamma$  enzyme. (b) Saturation curves of the  $\alpha\beta$  enzyme. (c) Saturation curves of the  $\alpha\gamma$  enzyme. The activities of the  $\alpha_2\beta\gamma$  and  $\alpha\gamma$  enzymes were measured at the standard conditions (33 mM Tris-acetate, pH 7.4, 2 mM  $\text{MnCl}_2$ , and 3.2 mM NAD) with varied concentration of ICT in the absence or presence of 1 mM CIT or/and 1 mM ADP. The activity of the  $\alpha\beta$  enzyme was measured at the standard conditions but with higher concentration of  $\text{Mn}^{2+}$  (50 mM). The derived  $V_{\max}$ ,  $S_{0.5}$  and  $k_{\text{cat}}$  are listed in Tables 2 and 3.

$\alpha_2\beta\gamma$  and  $\alpha\gamma$  enzymes contain at least two ICT-binding sites with positive cooperativity whereas the  $\alpha\beta$  enzyme contains only one ICT-binding site (Table 2). In the presence of CIT, ADP and both activators, the  $\alpha_2\beta\gamma$  enzyme still exhibits a Hill coefficient of 1.5, 2.0, and 1.5, respectively, indicating a cooperative binding for ICT in all these conditions; whereas the  $\alpha\gamma$  enzyme exhibits a Hill coefficient of 1.2, 1.6, and 1.0, respectively, indicating that there is a cooperative binding for ICT only in the absence of CIT (Table 3). As expected, the Hill coefficient of the  $\alpha\beta$  enzyme is not affected by CIT or/and ADP. These results suggest that the  $\alpha\gamma$  heterodimer may contain an ICT-binding site each in the  $\alpha$  and  $\gamma$  subunits; CIT appears to bind to one site most likely in the  $\gamma$  subunit and thus eliminates the positive cooperativity, but the ADP binding does not occlude the binding of ICT to this site and thus retains the cooperativity. The  $\alpha\beta$  enzyme contains only one ICT-binding site very likely in the  $\alpha$  subunit but no ICT-binding site in the  $\beta$  subunit. As the  $\alpha_2\beta\gamma$  enzyme exists as a dimer of heterotetramer, there is

Enzyme	+CIT			+ADP			+CIT+ADP				
	$V_{max,ICT}$	$S_{0.5,ICT}$	Hill coefficient for ICT	$V_{max,ICT}$	$S_{0.5,ICT}$	Hill coefficient for ICT	$V_{max,ICT}$	$S_{0.5,ICT}$	Hill coefficient for ICT	$k_{cat}^a$	$k_{cat}/S_{0.5,ICT}$
	$\mu\text{mol}/\text{mg}/\text{min}$	mM		$\mu\text{mol}/\text{mg}/\text{min}$	mM		$\mu\text{mol}/\text{mg}/\text{min}$	mM		$\text{s}^{-1}$	$\text{s}^{-1}\text{mM}^{-1}$
$\alpha_2\beta\gamma$	20.7 ± 1.3	1.27 ± 0.06	1.5 ± 0.1	22.1 ± 0.3	0.868 ± 0.021	2.0 ± 0.1	21.3 ± 0.4	0.163 ± 0.007	1.5 ± 0.1	28.4 ± 0.5	174 ± 3
$\alpha\beta$	11.2 ± 0.4	12.1 ± 1.1	1.1 ± 0.1	11.2 ± 0.3	12.1 ± 1.1	1.0 ± 0.1	11.9 ± 0.3	12.6 ± 0.8	1.2 ± 0.1	15.8 ± 0.4	1.25 ± 0.03
$\alpha\gamma$	10.0 ± 0.2	2.61 ± 0.12	1.2 ± 0.0	9.42 ± 0.09	1.69 ± 0.05	1.6 ± 0.1	13.1 ± 0.4	0.182 ± 0.015	1.0 ± 0.0	17.6 ± 0.5	96.7 ± 2.7

**Table 3. Kinetic parameters of the  $\alpha_2\beta\gamma$ ,  $\alpha\beta$  and  $\alpha\gamma$  enzymes in the presence of positive regulators.**

The  $V_{max,ICT}$  and  $S_{0.5,ICT}$  of the  $\alpha_2\beta\gamma$  and  $\alpha\gamma$  enzymes in the presence of 1 mM CIT or 1 mM ADP or both were determined at the standard conditions with varied concentrations of ICT. The  $V_{max,ICT}$  and  $S_{0.5,ICT}$  of the  $\alpha\beta$  enzyme were determined at the same conditions but with higher concentration of  $\text{MnCl}_2$  (50 mM) and varied concentrations of ICT. <sup>a</sup>A molecular mass of 80 kDa was used to calculate the mole of enzyme in heterodimeric form per mg of protein ( $1.25 \times 10^{-8}$  mol of dimeric enzyme/mg of protein).

a positive cooperative binding for ICT between the two heterotetramers or/and the  $\alpha\beta$  and  $\alpha\gamma$  heterodimers in both the absence and presence of regulators.

**Activation and inhibition of human NAD-IDH by ATP.** The previous biochemical data showed that the activities of mammalian NAD-IDHs can be negatively regulated by ATP<sup>1,11,20</sup>. To investigate the regulatory effect of ATP, we measured the activities of the  $\alpha_2\beta\gamma$ ,  $\alpha\beta$  and  $\alpha\gamma$  enzymes at different concentrations of ATP in the absence or presence of CIT or both CIT and ADP. Surprisingly, our results show that ATP has both activation and inhibition effects on the activities of the  $\alpha_2\beta\gamma$  and  $\alpha\gamma$  enzymes but only inhibition effect on the  $\alpha\beta$  enzyme (Fig. 3). For the  $\alpha_2\beta\gamma$  enzyme, ATP exhibits activation effect at low concentration with a maximum of 2.5-fold increase of the activity at [ATP] of 2 mM in the absence of any regulators, but exhibits inhibition effect at high concentration with no measurable activity at [ATP] of >3.5 mM (Fig. 3a). In the presence of CIT, the dependency of the activity on the ATP concentration displays a similar pattern with a maximum of 9-fold increase of the activity at [ATP] of 1 mM and a complete inhibition at [ATP] of >4 mM. In the presence of CIT and ADP, the  $\alpha_2\beta\gamma$  enzyme has been fully activated, and thus ATP exhibits no activation effect but only inhibition effect on the activity at [ATP] of >1 mM with a complete inhibition at [ATP] of >8 mM. Similar to the  $\alpha_2\beta\gamma$  enzyme, the activity of the  $\alpha\gamma$  enzyme is slightly activated in the absence of CIT and significantly activated in the presence of CIT by low concentration of ATP, but is inhibited by high concentration of ATP; and additionally ATP exhibits only inhibition effect at [ATP] of >1 mM in the presence of CIT and ADP (Fig. 3c). In contrast, the activity of the  $\alpha\beta$  enzyme is completely inhibited by ATP even at low concentration in either absence or presence of CIT or CIT and ADP (Fig. 3b).

As the  $\alpha_2\beta\gamma$  and  $\alpha\gamma$  enzymes display higher activities in the presence of low ATP concentration, we further analyzed the effects of ATP on the kinetic parameters of these enzymes in the presence of ATP or CIT and ATP (Table 4). Compared to those in the absence of any regulators, the  $V_{max,ICT}$  of the  $\alpha_2\beta\gamma$  enzyme is not significantly affected by ATP or CIT and ATP, but the  $S_{0.5,ICT}$  is slightly decreased by 2.8-fold in the presence of ATP and substantially decreased by 12.2-fold in the presence of CIT and ATP. Similarly, the  $V_{max,ICT}$  of the  $\alpha\gamma$  enzyme is also not significantly affected by ATP or CIT and ATP, but the  $S_{0.5,ICT}$  is decreased by 1.5-fold in the presence of ATP and by 14.5-fold in the presence of CIT and ATP. Consistently, the  $\alpha_2\beta\gamma$  enzyme exhibits positive cooperativity for ICT binding with a Hill coefficient of 1.8 and 1.4 in the presence of ATP and both CIT and ATP, respectively; and the  $\alpha\gamma$  enzyme exhibits positive cooperativity with a Hill coefficient of 1.4 in the presence of ATP but no cooperativity in the presence of both CIT and ATP (Table 4). To avoid that the activation effect of ATP is due to contamination of ADP or hydrolyzation of ATP into ADP, we used the nonhydrolyzable ATP analogue AMP-PNP to perform the same assays, and similar activation and inhibition effects are observed (Supplementary Table S2 and Figure S1). These results indicate that ATP can activate the  $\alpha_2\beta\gamma$  and  $\alpha\gamma$  enzymes at low concentration but inhibit their activities at high concentration, whereas ATP exhibits only inhibition effect on the  $\alpha\beta$  enzyme. The activation of the  $\alpha_2\beta\gamma$  and  $\alpha\gamma$  enzymes by low concentration of ATP is in a similar manner as ADP but with a slightly weaker effect.

**The  $\gamma$  subunit regulates both the  $\alpha\beta$  and  $\alpha\gamma$  heterodimers in the holoenzyme.** Our biochemical data show that the full activity of the  $\alpha_2\beta\gamma$  heterotetramer requires the assembly and cooperative functions of the  $\alpha\beta$  and  $\alpha\gamma$  heterodimers in both the absence and presence of activators. The previous biochemical data showed that mutation of  $\alpha$ -Tyr126 to Phe, Ser or Glu completely abolishes the activity of the  $\alpha_2\beta\gamma$  holoenzyme<sup>23</sup>. To investigate the functional roles of the  $\beta$  and  $\gamma$  subunits and the  $\alpha\beta$  and  $\alpha\gamma$  heterodimers in the  $\alpha_2\beta\gamma$  heterotetramer, we introduced the  $\alpha$ -Y126F mutation into the  $\alpha\beta$  and  $\alpha\gamma$  heterodimers separately, and expressed and purified the mutant  $\alpha_{Y126F}\beta$  and  $\alpha_{Y126F}\gamma$  heterodimers. The mutant  $\alpha_{Y126F}\beta\alpha\gamma$  heterotetramer was assembled by mixing the purified  $\alpha_{Y126F}\beta$  and  $\alpha\gamma$  proteins with 1:1 molar ratio, and the mutant  $\alpha\beta\alpha_{Y126F}\gamma$  heterotetramer was assembled by mixing the purified  $\alpha\beta$  and  $\alpha_{Y126F}\gamma$  proteins with 1:1 molar ratio followed by purification using gel filtration. SEC-MALS analyses indicate that introduction of the  $\alpha$ -Y126F mutation does not affect the oligomeric states of the  $\alpha\beta$ ,  $\alpha\gamma$  and  $\alpha_2\beta\gamma$  proteins in solution: like the wild-type proteins, the mutant  $\alpha_{Y126F}\beta\alpha\gamma$  and  $\alpha\beta\alpha_{Y126F}\gamma$  proteins exist as heterooctamers, and the mutant  $\alpha_{Y126F}\beta$  and  $\alpha_{Y126F}\gamma$  proteins exist as heterodimers at low concentration but as dimers of heterodimers at high concentration (Supplementary Figure S2). As expected, the

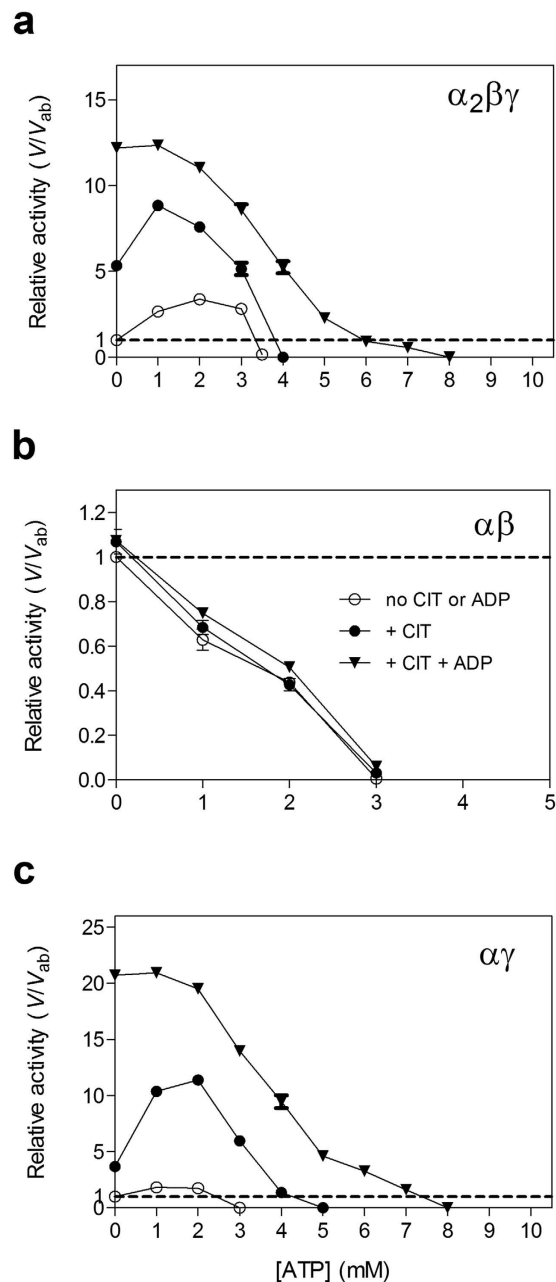


**Figure 3. Activation and inhibition effects of ATP.** (a) The relative activity of the  $\alpha_2\beta\gamma$  enzyme vs. the concentration of ATP in the absence or presence of positive regulator(s). (b) The relative activity of the  $\alpha\beta$  enzyme vs. the concentration of ATP in the absence or presence of positive regulator(s). (c) The relative activity of the  $\alpha\gamma$  enzyme vs. the concentration of ATP in the absence or presence of positive regulator(s). The activities in the absence of any regulators ( $V_{ab}$ ) are defined as 1 and indicated by dashed lines. The activities were measured at the standard conditions with a subsaturating concentration of ICT (0.6 mM for the  $\alpha_2\beta\gamma$  and  $\alpha\gamma$  enzymes and 2 mM for the  $\alpha\beta$  enzyme) in the absence or presence of 1 mM CIT or/and 1 mM ADP and varied concentration of ATP (0–10 mM).

mutant  $\alpha_{Y126F}\beta$  and  $\alpha_{Y126F}\gamma$  heterodimers and the mutant  $\alpha_{Y126F}\beta\alpha_{Y126F}\gamma$  heterotetramer have no detectable activity (Table 5). Intriguingly, the mutant  $\alpha_{Y126F}\beta\alpha\gamma$  and  $\alpha\beta\alpha_{Y126F}\gamma$  heterotetramers exhibit comparable  $S_{0.5,ICT}$  and about half of the catalytic efficiency compared with the wild-type holoenzyme in both the absence and presence of CIT and ADP, indicating that both  $\alpha\beta$  and  $\alpha\gamma$  heterodimers in the  $\alpha_2\beta\gamma$  heterotetramer can be activated by the activators and contribute equally to the full activity of the holoenzyme. On the other hand, our kinetic data show that only the  $\alpha\gamma$  heterodimer alone can be activated by the activators whereas the  $\alpha\beta$  heterodimer alone cannot. These results led us to speculate that both  $\alpha\beta$  and  $\alpha\gamma$  heterodimers in the holoenzyme might be regulated by the  $\gamma$  subunit. Meanwhile, our structural and biochemical studies show that the positive regulation of the  $\alpha\gamma$  heterodimer by CIT and ADP is through their binding to the allosteric site in the  $\gamma$  subunit which causes conformational

Enzyme	+ATP			+CIT+ATP				
	$V_{\max,ICT}$	$S_{0.5,ICT}$	Hill coefficient for ICT	$V_{\max,ICT}$	$S_{0.5,ICT}$	Hill coefficient for ICT	$k_{cat}^a$	$k_{cat}/S_{0.5,ICT}$
	$\mu\text{mol}/\text{mg}/\text{min}$	$\text{mM}$		$\mu\text{mol}/\text{mg}/\text{min}$	$\text{mM}$		$\text{s}^{-1}$	$\text{s}^{-1}\text{mM}^{-1}$
$\alpha_2\beta\gamma$	$17.7 \pm 0.1$	$0.825 \pm 0.021$	$1.8 \pm 0.1$	$17.6 \pm 0.1$	$0.193 \pm 0.005$	$1.4 \pm 0.0$	$23.4 \pm 0.1$	$121 \pm 1$
$\alpha\gamma$	$6.62 \pm 0.19$	$2.98 \pm 0.16$	$1.4 \pm 0.1$	$8.94 \pm 0.36$	$0.309 \pm 0.014$	$1.1 \pm 0.0$	$11.9 \pm 0.5$	$38.5 \pm 1.6$

**Table 4. Kinetic parameters of the  $\alpha_2\beta\gamma$  and  $\alpha\gamma$  enzymes in the presence of ATP or both CIT and ATP.**

The  $V_{\max,ICT}$  and  $S_{0.5,ICT}$  in the presence of 1 mM ATP or both 1 mM CIT and 1 mM ATP were determined at the standard conditions with varied concentrations of ICT. <sup>a</sup>A molecular mass of 80 kDa was used to calculate the mole of enzyme in heterodimeric form per mg of protein ( $1.25 \times 10^{-8}$  mol of dimeric enzyme/mg of protein).

changes at both the allosteric site and the active site<sup>39</sup>. The  $\gamma$ -K151A mutation disrupts the structural communication between the allosteric site and the active site and thus abolishes the activation of the  $\alpha\gamma$  enzyme by CIT and ADP<sup>39</sup>. Thus, we prepared the mutant  $\alpha\beta\alpha\gamma_{K151A}$  heterotetramer and carried out kinetic study. Indeed, this mutant holoenzyme has very low activity and cannot be activated by CIT and ADP (Table 5). In addition, our kinetic data show that the mutant  $\alpha_{Y126F}\beta\alpha\gamma$  and  $\alpha\beta\alpha_{Y126F}\gamma$  holoenzymes exhibit a Hill coefficient of 1.6–1.7 in the absence of the activators and a Hill coefficient of 1.3–1.4 in the presence of the activators, indicating that there is a cooperative binding for ICT in the absence and presence of the activators. However, the mutant  $\alpha\beta\alpha\gamma_{K151A}$  holoenzyme exhibits a Hill coefficient of 1.0 in both the absence and presence of the activators, indicating that there is no cooperative binding for ICT. These results together indicate that the  $\gamma$  subunit plays a critical role in the allosteric regulation of the holoenzyme and can regulate both the  $\alpha\beta$  and  $\alpha\gamma$  heterodimers in the  $\alpha_2\beta\gamma$  heterotetramer.

## Discussion

Human NAD-IDH is an allosteric enzyme consisting of the  $\alpha\beta$  and  $\alpha\gamma$  heterodimers that are assembled into the  $\alpha_2\beta\gamma$  heterotetramer and further into the heterooctamer. The previous biochemical studies showed that the  $\alpha$  subunit plays the catalytic role and the  $\beta$  and  $\gamma$  subunits the regulatory roles<sup>19,22–25</sup>. However, the enzymatic properties of the composing  $\alpha\beta$  and  $\alpha\gamma$  heterodimers are not well studied and the exact functional roles of the  $\beta$  and  $\gamma$  subunits in the  $\alpha_2\beta\gamma$  heterotetramer are still elusive. In this work, we systematically characterized the enzymatic properties of the  $\alpha_2\beta\gamma$  heterotetramer and the  $\alpha\beta$  and  $\alpha\gamma$  heterodimers in the absence and presence of different regulators, which reveal new mechanistic insights into the function and allosteric regulation of human NAD-IDH.

Our biochemical data show that the  $\alpha_2\beta\gamma$  enzyme has basal activity in the absence of any regulators, and can be slightly activated by CIT or ADP alone but substantially activated by CIT and ADP together, indicating that the two activators work synergistically. The binding of CIT or/and ADP enhances the catalytic efficiency of the enzyme by decreasing the  $S_{0.5,ICT}$  but has no significant effect on the  $V_{\max,ICT}$ . In addition, the  $\alpha_2\beta\gamma$  enzyme exhibits cooperative binding for ICT in both the absence and presence of CIT or/and ADP. These data indicate that the  $\alpha_2\beta\gamma$  enzyme contains at least two ICT-binding sites with positive cooperativity, and CIT and ADP have distinct binding sites and can bind to the enzyme independently and simultaneously in a synergistic manner.

The  $\alpha\gamma$  heterodimer alone exhibits similar kinetic properties as the  $\alpha_2\beta\gamma$  enzyme in both the absence and presence of the activator(s) and can also be activated by CIT or/and ADP in similar manners. In the presence of CIT and ADP, the  $S_{0.5,ICT}$  of the  $\alpha\gamma$  enzyme is decreased by 24.7-fold and the catalytic efficiency is increased by 44.8-fold which is elevated from 19.0% (in the absence of activators) to 55.6% of that of the  $\alpha_2\beta\gamma$  enzyme. Moreover, our kinetic data show that the  $\alpha\gamma$  enzyme exhibits cooperative binding for ICT in the absence of any activators and in the presence of ADP, but no cooperative binding in the presence of CIT or both CIT and ADP, suggesting that the  $\alpha\gamma$  enzyme contains two ICT-binding sites probably with one each in the  $\alpha$  and  $\gamma$  subunits; CIT binds to one ICT-binding site most likely in the  $\gamma$  subunit and the ADP binding does not occlude the binding of ICT or CIT to this site. These results are consistent with and supported by our structural and biochemical data showing that the  $\alpha\gamma$  heterodimer contains the allosteric site in the  $\gamma$  subunit which is consisted of a CIT-binding site and an ADP-binding site, and the binding of CIT (and ADP) causes conformational changes at the allosteric site which are transmitted to the active site in the  $\alpha$  subunit through a cascade of conformational changes at the heterodimer interface, leading to stabilization of the ICT binding at the active site and thus activation of the enzyme<sup>39</sup>. In addition, our mutagenesis data show that mutation of a key residue in the  $\gamma$  subunit ( $\gamma$ -K151A) completely abolishes the activation effect of the holoenzyme. These data together indicate that the  $\gamma$  subunit plays the regulatory role in the  $\alpha\gamma$  heterodimer and  $\alpha_2\beta\gamma$  holoenzyme.

In contrast, the  $\alpha\beta$  enzyme exhibits kinetic properties dissimilar to the  $\alpha\gamma$  and  $\alpha_2\beta\gamma$  enzymes and has significantly higher  $S_{0.5}$  values for ICT and  $\text{Mn}^{2+}$  in both the absence and presence of the activator(s). The  $\alpha\beta$  enzyme cannot be activated by CIT or/and ADP, and the catalytic efficiency is about 9.5% of that of the  $\alpha_2\beta\gamma$  enzyme at high concentration of  $\text{Mn}^{2+}$  in the absence of the activator(s) and about 0.7% of that of the  $\alpha_2\beta\gamma$  enzyme in the presence of CIT and ADP. In addition, the  $\alpha\beta$  enzyme exhibits no cooperative binding for ICT in both the absence and presence of the activator(s). These data suggest that the  $\alpha\beta$  enzyme contains only one ICT-binding site most likely in the  $\alpha$  subunit and no allosteric site in the  $\beta$  subunit. These results are also consistent with and supported by our structural and biochemical data showing that the  $\alpha\beta$  enzyme contains no allosteric site in the  $\beta$  subunit and cannot bind CIT or/and ADP due to structural and conformational differences at the “pseudo” allosteric site (Ma *et al.*, unpublished data). Nevertheless, our mutagenesis data with the holoenzyme show that



Enzyme	Specific activity $\mu\text{mol}/\text{mg}/\text{min}$	No activators				CIT+ADP			
		$V_{\text{max,ICT}}$	$S_{0.5,\text{ICT}}$	$k_{\text{cat}}^2/S_{0.5,\text{ICT}}$	Hill coefficient for ICT	$V_{\text{max,ICT}}$	$S_{0.5,\text{ICT}}$	$k_{\text{cat}}/S_{0.5,\text{ICT}}$	Hill coefficient for ICT
		$\mu\text{mol}/\text{mg}/\text{min}$	mM	$\text{s}^{-1}\text{mM}^{-1}$		$\mu\text{mol}/\text{mg}/\text{min}$	mM	$\text{s}^{-1}\text{mM}^{-1}$	
$\alpha\beta\alpha\gamma$	$20.2 \pm 0.3$	$20.0 \pm 0.1$	$2.35 \pm 0.05$	$11.36 \pm 0.04$	$2.0 \pm 0.1$	$21.3 \pm 0.4$	$0.163 \pm 0.007$	$174 \pm 3$	$1.5 \pm 0.1$
$\alpha_{Y126F}\beta$	0	ND <sup>c</sup>	ND	ND	ND	ND	ND	ND	ND
$\alpha_{Y126F}\gamma$	0	ND	ND	ND	ND	ND	ND	ND	ND
$\alpha_{Y126F}\beta\alpha_{Y126F}\gamma$	0	ND	ND	ND	ND	ND	ND	ND	ND
$\alpha\beta\alpha_{Y126F}\gamma$	$8.45 \pm 0.14$	$8.47 \pm 0.42$	$2.12 \pm 0.13$	$5.32 \pm 0.13$	$1.6 \pm 0.1$	$8.43 \pm 0.32$	$0.148 \pm 0.005$	$75.9 \pm 5.1$	$1.4 \pm 0.1$
$\alpha_{Y126F}\beta\alpha\gamma$	$9.00 \pm 0.15$	$9.07 \pm 0.39$	$2.41 \pm 0.12$	$5.02 \pm 0.12$	$1.7 \pm 0.1$	$9.12 \pm 0.39$	$0.129 \pm 0.006$	$94.2 \pm 3.0$	$1.3 \pm 0.1$
$\alpha\beta\alpha_{K151A}$ <sup>b</sup>	$1.76 \pm 0.11$	$8.24 \pm 0.59$	$21.9 \pm 1.1$	$0.501 \pm 0.035$	$1.0 \pm 0.1$	$8.02 \pm 0.42$	$17.6 \pm 1.5$	$0.607 \pm 0.032$	$1.0 \pm 0.1$

**Table 5. Kinetic parameters of the mutant holoenzyme.** The  $V_{\text{max,ICT}}$  and  $S_{0.5,\text{ICT}}$  in the absence or presence of both 1 mM CIT and 1 mM ADP were determined at the standard conditions with varied concentrations of ICT, except for those noted specifically. <sup>a</sup>A molecular mass of 80 kDa was used to calculate the mole of enzyme in heterodimeric form per mg of protein ( $1.25 \times 10^{-8}$  mol of dimeric enzyme/mg of protein). <sup>b</sup>The mutant  $\alpha\beta\alpha_{K151A}$  enzyme has the  $S_{0.5,\text{Mn}}$  and  $S_{0.5,\text{NAD}}$  of  $5.10 \pm 0.46$  mM and  $1.54 \pm 0.27$  mM, respectively, which are much higher than those of the wild-type enzyme. Thus, the  $V_{\text{max,ICT}}$  and  $S_{0.5,\text{ICT}}$  were determined at higher concentrations of  $\text{MnCl}_2$  (50 mM) and NAD (10 mM). <sup>c</sup>ND: not detectable.

the  $\alpha\beta$  heterodimer also contributes to the full activity of the holoenzyme in both the absence and presence of the activators, and can be activated by CIT and ADP through the  $\gamma$  subunit. These data together suggest that the  $\beta$  subunit plays a structural role in the  $\alpha_2\beta\gamma$  heterotetramer to facilitate the assembly and thus ensure the full activity of the holoenzyme. The previous biochemical data showed that several residues of the  $\beta$  subunit, including  $\beta$ -Arg99,  $\beta$ -Tyr137,  $\beta$ -Asp192 and  $\beta$ -Asp217, play important roles in the function and regulation of the  $\alpha_2\beta\gamma$  enzyme<sup>19,23–25</sup>. Our mutagenesis and biochemical data show that although these mutations have no effect on the basal activity of the  $\alpha\beta$  enzyme, some of them at the heterodimer interface have some effects on the activity of the  $\alpha_2\beta\gamma$  enzyme in the absence and particularly in the presence of the activators (Ma *et al.*, unpublished data). It is very likely that the  $\beta$  subunit is involved in the heterodimer-heterodimer and/or heterotetramer-heterotetramer interfaces in the holoenzyme, and the conformational changes at the allosteric site in the  $\gamma$  subunit induced by the binding of activators are transmitted to the active sites in the  $\alpha\gamma$  and  $\alpha\beta$  heterodimers via the interfaces, and thus mutations of the  $\beta$  subunit at the heterodimer interface would affect the cooperative function(s) of the two heterodimers and/or heterotetramers and hence compromise the full activity of the holoenzyme.

Surprisingly, our biochemical data show that ATP has both activation and inhibition effects on the  $\alpha_2\beta\gamma$  and  $\alpha\gamma$  enzymes dependent on the concentration but only inhibition effect on the  $\alpha\beta$  enzyme, which are different from the previous biochemical data showing that ATP only inhibits the activity of bovine heart NAD-IDH<sup>11</sup>. In the absence of any activators or the presence of CIT, ATP can activate the  $\alpha_2\beta\gamma$  and  $\alpha\gamma$  enzymes at low concentration but inhibit their activities at high concentration. In the presence of both CIT and ADP, ATP exhibits only inhibition effect on the activities as the enzymes have been fully activated. Moreover, our kinetic data show that the activation effect of ATP is exerted in a similar manner as ADP. These results lead us to speculate that there might be two different binding sites for ATP in the  $\alpha_2\beta\gamma$  and  $\alpha\gamma$  enzymes. One binding site might be the same site for ADP in the  $\gamma$  subunit and the binding of ATP to this site could positively regulate the activity in a synergistic manner with CIT. Indeed, our preliminary structural data show that ATP can bind to the ADP-binding site of the  $\alpha\gamma$  heterodimer in the presence of CIT, which can induce similar conformational changes as the binding of CIT and ADP (Ma *et al.*, unpublished data). The other binding site might be at the active site, as suggested earlier<sup>11</sup>, and the binding of ATP to this site would compete with the NAD binding and thus inhibits the activity. It is also possible that high concentration of ATP may compete for binding with the metal ion and thus confers inhibition on the activity. More biochemical and structural studies are needed to dissect the molecular mechanism of the dual effect of ATP.

Taken together, our biochemical data indicate that the  $\alpha\beta$  and  $\alpha\gamma$  enzymes alone have considerable basal activities but exhibit different enzymatic properties: the  $\alpha\gamma$  enzyme shares very similar kinetic characteristics and allosteric regulation patterns as the  $\alpha_2\beta\gamma$  enzyme, whereas the  $\alpha\beta$  enzyme does not. Both the  $\alpha\beta$  and  $\alpha\gamma$  heterodimers in the  $\alpha_2\beta\gamma$  heterotetramer contribute equally to the full activity of the holoenzyme in both the absence and presence of the activators, and the positive regulation of the  $\alpha\beta$  and  $\alpha\gamma$  heterodimers in the  $\alpha_2\beta\gamma$  heterotetramer is through the  $\gamma$  subunit but not the  $\beta$  subunit. These results together demonstrate that the  $\alpha$  subunits play the catalytic role, the  $\gamma$  subunit the regulatory role, and the  $\beta$  subunit the structural role in the  $\alpha_2\beta\gamma$  heterotetramer. Further biochemical and structural studies of the  $\alpha_2\beta\gamma$  heterotetramer will provide more insights into the molecular basis of the specific functional roles of the  $\beta$  and  $\gamma$  subunits and the  $\alpha\beta$  and  $\alpha\gamma$  heterodimers in the  $\alpha_2\beta\gamma$  heterotetramer and reveal the catalytic and regulatory mechanisms of the  $\alpha_2\beta\gamma$  heterotetramer.

## Methods

**Cloning, expression, and purification.** The  $\alpha\beta$  and  $\alpha\gamma$  heterodimers and the  $\alpha_2\beta\gamma$  heterotetramer of human NAD-IDH were prepared using a method different from that described previously<sup>22</sup>. Human *IDH3A*, *IDH3B* (isoform 2), and *IDH3G* genes in vector pReceiver-B01/B02 were purchased from FugenGen (China). The N-terminal 27, 34 and 39 residues of the  $\alpha$ ,  $\beta$  and  $\gamma$  subunits, respectively, which are the signal peptides for their translocation into the mitochondria<sup>40</sup>, were removed during construction. The DNA fragments of the  $\alpha$ ,  $\beta$  and

$\gamma$  subunits were individually cloned into the co-expression vector pQlinkN with the C-terminals of the  $\beta$  and  $\gamma$  subunits attached with or without a TEV protease cleavage site and a His<sub>6</sub> tag, which were then used to construct the pQlinkN- $\alpha$ - $\beta$ -tev-His<sub>6</sub>, pQlinkN- $\alpha$ - $\gamma$ -tev-His<sub>6</sub>, pQlinkN- $\alpha$ - $\beta$ , and pQlinkN- $\alpha$ - $\gamma$  plasmids, and subsequently the pQlinkN- $\alpha$ - $\gamma$ - $\alpha$ - $\beta$ -tev-His<sub>6</sub> plasmid, following the pQlink cloning procedure<sup>41</sup>.

The pQlinkN- $\alpha$ - $\beta$ -tev-His<sub>6</sub> and pQlinkN- $\alpha$ - $\gamma$ -tev-His<sub>6</sub> plasmids were transformed into *E. coli* BL21 (DE3) Codon-Plus strain (Novagen) for expressions of the  $\alpha\beta$  and  $\alpha\gamma$  heterodimers, and the pQlinkN- $\alpha$ - $\gamma$ - $\alpha$ - $\beta$ -tev-His<sub>6</sub> plasmid for expression of the  $\alpha_2\beta\gamma$  heterotetramer. When the culture of the transformed cells reached an OD<sub>600</sub> of 0.4–0.6, the protein expression was induced by 0.4 mM IPTG for 20 hr at 23 °C. The bacterial cells were harvested, resuspended, and sonicated on ice in a lysis buffer (50 mM HEPES-Na, pH 7.4, 200 mM NaCl, 0.2 mM MnCl<sub>2</sub>, 10% (w/v) glycerol, and 7.2 mM  $\beta$ -ME) supplemented with 1 mM PMSF. The target protein was firstly purified by affinity chromatography using a Ni-NTA column (Qiagen) with the lysis buffer supplemented with 20 mM and 200 mM imidazole serving as the washing buffer and elution buffer, respectively. The elution fraction was dialyzed against the lysis buffer overnight to lower the concentration of imidazole to < 10 mM; meanwhile, the His<sub>6</sub>-tag was cleaved by TEV protease. The protein mixture was reloaded on a Ni-NTA column, which was then washed with the lysis buffer supplemented with 10 mM imidazole. The flow-through fraction containing the target protein was concentrated by centrifugation using an Amicon Ultra-4 centrifugal filter unit with Ultracel-30 membrane (Millipore), and then purified by gel filtration using a Superdex 200 10/300 GL column (GE Healthcare) equilibrated with the storage buffer (10 mM HEPES, pH 7.4, 200 mM NaCl, and 5 mM  $\beta$ -ME). As the yield of the co-expressed  $\alpha_2\beta\gamma$  heterotetramer was much lower than those of the  $\alpha\beta$  and  $\alpha\gamma$  heterodimers, we assembled the  $\alpha_2\beta\gamma$  heterotetramer by either co-purifying the separately expressed  $\alpha\beta$  and  $\alpha\gamma$  heterodimers using a combination of affinity chromatography and gel filtration, or mixing the purified  $\alpha\beta$  and  $\alpha\gamma$  heterodimers at 1:1 molar ratio overnight followed by purification using gel filtration chromatography. Both methods produced the  $\alpha_2\beta\gamma$  heterotetramer with much higher yields. Purities of the protein samples were assessed by 12% SDS-PAGE with Coomassie blue staining. Concentrations of the proteins were determined using the BCA Protein Assay Kit (Thermo Scientific). Mutants of the  $\alpha\beta$  and  $\alpha\gamma$  heterodimers containing point mutations in the  $\alpha$ ,  $\beta$  and  $\gamma$  subunits were constructed using the QuikChange<sup>®</sup> Site-Directed Mutagenesis kit (Stratagene). Expression and purification of the mutants were carried out the same as for the wild-type proteins.

**SEC-MALS analysis.** The purity, molecular mass and size distribution of the proteins were analyzed by an analytical light scattering instrument (SEC-MALS) consisting of an Agilent 1260 Infinity Isocratic Liquid Chromatography System, a Wyatt Dawn Heleos II Multi-Angle Light Scattering Detector (Wyatt Technology) and a Wyatt Optilab T-rEX Refractive Index Detector (Wyatt Technology). Analytical size exclusion chromatography was performed at room temperature using a Superdex 200 10/300 GL column (GE Healthcare) equilibrated with a mobile phase containing 10 mM HEPES (pH 7.4), 200 mM NaCl, and 5 mM  $\beta$ -ME. 100  $\mu$ l protein sample at concentration of 2 mg/ml or 12 mg/ml was injected into the column and eluted at a flow rate of 0.4 ml/min. The column effluent was monitored in-line with three detectors that simultaneously monitor the UV absorption, light scattering and refractive index. The measurements were analyzed using the ASTRA software (Wyatt Technology) to determine the molecular mass of the protein<sup>42</sup>.

**Enzymatic activity assay.** The activities of the  $\alpha_2\beta\gamma$ ,  $\alpha\beta$  and  $\alpha\gamma$  enzymes were determined by monitoring the time-dependent formation of NADH at 340 nm ( $\epsilon = 6220 \text{ M}^{-1} \text{ cm}^{-1}$ ) using a Coulter DU 800 Spectrophotometer (Beckman) at 25 °C. The standard reaction solution (1 ml) consisted of 33 mM Tris-acetate (pH 7.4), 2 ng/ml enzyme, 80 mM DL-isocitrate, 2 mM MnCl<sub>2</sub>, and 3.2 mM NAD. The catalytic reaction was initiated by addition of NAD. The specific activity is defined as the amount of NADH produced per minute per milligram of enzyme ( $\mu\text{mol}/\text{min}/\text{mg}$ ).

The kinetic parameters of the enzymes in the absence of regulators were determined at the standard conditions with varied concentrations of ICT (0–80 mM), Mn<sup>2+</sup> (0–2 mM), or NAD (0–3.2 mM) to obtain the  $V_{\text{max}}$  and the  $S_{0.5}$  for ICT, Mn<sup>2+</sup>, or NAD, respectively. As the  $\alpha\beta$  enzyme had low activity and very high  $S_{0.5,\text{Mn}}$  at the standard conditions, its kinetic parameters were measured at the conditions with substantially increased concentration of MnCl<sub>2</sub> (50 mM). The kinetic parameters in the presence of regulators were determined at the standard conditions containing 1 mM CIT or 1 mM ADP (ATP), or both. The production of NADH follows pseudo-first-order kinetics and the time course of the product appearance is well modeled by a linear function up to the time when about 10% of the total substrate was converted to the product. The initial rate was determined from the slope of a linear fit of the early time point data. The kinetic parameters were obtained by fitting the experimental data into the non-Michaelis-Menten equation “ $V = V_{\text{max}} * [S]^h / (S_{0.5}^h + [S]^h)$ ” using the program Graphpad Prism (Graphpad Software), where “h” is the Hill coefficient, “ $S_{0.5}$ ” is the apparent  $K_m$  (the substrate concentration at the reaction velocity of  $0.5 * V_{\text{max}}$ ), and “[S]” is the concentration of ICT, Mn<sup>2+</sup>, or NAD. All the experiments were performed in three independent measurements and the values were the averages of the three measurements with the standard errors.

For determination of the effect of ATP, the activities of the enzymes were measured at the standard conditions except for a subsaturating concentration of ICT (0.6 mM for the  $\alpha_2\beta\gamma$  and  $\alpha\gamma$  enzymes and 2 mM for the  $\alpha\beta$  enzyme) and varied concentrations of ATP (0–10 mM).

## References

- McAlister-Henn, L. Ligand binding and structural changes associated with allostery in yeast NAD(+)-specific isocitrate dehydrogenase. *Arch Biochem Biophys* **519**, 112–117 (2012).
- Ehrlich, R. S. & Colman, R. Separation, recombination, and characterization of dissimilar subunits of the DPN-dependent isocitrate dehydrogenase from pig heart. *J Biol Chem* **258**, 7079–7086 (1983).

3. Ehrlich, R. S., Hayman, S., Ramachandran, N. & Colman, R. Re-evaluation of molecular weight of pig heart NAD-specific isocitrate dehydrogenase. *J Biol Chem* **256**, 10560–10564 (1981).
4. Ehrlich, R. S. & Colman, R. F. Interrelationships among nucleotide binding sites of pig heart NAD-dependent isocitrate dehydrogenase. *J Biol Chem* **257**, 4769–4774 (1982).
5. Ramachandran, N. & Colman, R. F. Chemical characterization of distinct subunits of pig heart DPN-specific isocitrate dehydrogenase. *J Biol Chem* **255**, 8859–8864 (1980).
6. Cohen, P. F. & Colman, R. F. Purification of NAD-specific isocitrate dehydrogenase from porcine heart. *Biochim Biophys Acta* **242**, 325–330 (1971).
7. Cohen, P. F. & Colman, R. F. Diphosphopyridine nucleotide dependent isocitrate dehydrogenase from pig heart. Characterization of the active substrate and modes of regulation. *Biochemistry* **11**, 1501–1508 (1972).
8. Huang, Y. C., Kumar, A. & Colman, R. F. Identification of the subunits and target peptides of pig heart NAD-specific isocitrate dehydrogenase modified by the affinity label 8-(4-bromo-2,3-dioxobutylthio)NAD. *Arch Biochem Biophys* **348**, 207–218 (1997).
9. Plaut, G. W. & Aogaichi, T. Purification and properties of diphosphopyridine nucleotide-linked isocitrate dehydrogenase of mammalian liver. *J Biol Chem* **243**, 5572–5583 (1968).
10. Plaut, G. W., Schramm, V. L. & Aogaichi, T. Action of magnesium ion on diphosphopyridine nucleotide-linked isocitrate dehydrogenase from bovine heart. Characterization of the forms of the substrate and the modifier of the reaction. *J Biol Chem* **249**, 1848–1856 (1974).
11. Chen, R. F. & Plaut, G. Activation and inhibition of DPN-linked isocitrate dehydrogenase of heart by certain nucleotides. *Biochemistry* **2**, 1023–1032 (1963).
12. Plaut, G. W., Cheung, C. P., Suhadolnik, R. J. & Aogaichi, T. Cosubstrate and allosteric modifier activities of structural analogues of NAD and ADP for NAD-specific isocitrate dehydrogenase from bovine heart. *Biochemistry* **18**, 3430–3438 (1979).
13. Willson, V. J. & Tipton, K. F. The effect of ligands on the irreversible inhibition of the NAD<sup>+</sup>-dependent isocitrate dehydrogenase from ox brain. *Eur J Biochem* **117**, 65–68 (1981).
14. Nichols, B. J., Hall, L., Perry, A. C. & Denton, R. M. Molecular cloning and deduced amino acid sequences of the gamma-subunits of rat and monkey NAD(+)-isocitrate dehydrogenases. *Biochem J* **295** (Pt 2), 347–350 (1993).
15. Nichols, B. J., Perry, A. C., Hall, L. & Denton, R. M. Molecular cloning and deduced amino acid sequences of the alpha- and beta-subunits of mammalian NAD(+)-isocitrate dehydrogenase. *Biochem J* **310** (Pt 3), 917–922 (1995).
16. Cohen, P. F. & Colman, R. F. Role of manganous ion in the kinetics of pig-heart NAD-specific isocitrate dehydrogenase. *Eur J Biochem* **47**, 35–45 (1974).
17. Ehrlich, R. S. & Colman, R. F. Conformations of the coenzymes and the allosteric activator, ADP, bound to NAD(+)-dependent isocitrate dehydrogenase from pig heart. *Biochemistry* **29**, 5179–5187 (1990).
18. Ehrlich, R. S. & Colman, R. F. Cadmium-113 and magnesium-25 NMR study of the divalent metal binding sites of isocitrate dehydrogenases from pig heart. *Biochim Biophys Acta* **1246**, 135–141 (1995).
19. Soundar, S., O'Hagan, M., Fomulu, K. S. & Colman, R. F. Identification of Mn<sup>2+</sup>-binding aspartates from  $\alpha$ ,  $\beta$ , and  $\gamma$  subunits of human NAD-dependent isocitrate dehydrogenase. *J Biol Chem* **281**, 21073–21081 (2006).
20. Gabriel, J. & Plaut, G. Citrate activation of NAD-specific isocitrate dehydrogenase from bovine heart. *J Biol Chem* **259**, 1622–1628 (1984).
21. Ehrlich, R. S. & Colman, R. F. Binding of ligands to half of subunits of NAD-dependent isocitrate dehydrogenase from pig heart. Binding of manganous ion, isocitrate, ADP and NAD. *J Biol Chem* **256**, 1276–1282 (1981).
22. Kim, Y. O. *et al.* Identification and functional characterization of a novel, tissue-specific NAD(+)-dependent isocitrate dehydrogenase beta subunit isoform. *J Biol Chem* **274**, 36866–36875 (1999).
23. Dange, M. & Colman, R. F. Each conserved active site tyr in the three subunits of human isocitrate dehydrogenase has a different function. *J Biol Chem* **285**, 20520–20525 (2010).
24. Bzymek, K. P. & Colman, R. F. Role of  $\alpha$ -Asp181,  $\beta$ -Asp192, and  $\gamma$ -Asp190 in the distinctive subunits of human NAD-specific isocitrate dehydrogenase. *Biochemistry* **46**, 5391–5397 (2007).
25. Soundar, S., Park, J.-H., Huh, T.-L. & Colman, R. F. Evaluation by mutagenesis of the importance of 3 arginines in  $\alpha$ ,  $\beta$ , and  $\gamma$  subunits of human NAD-dependent isocitrate dehydrogenase. *J Biol Chem* **278**, 52146–52153 (2003).
26. Taylor, A. B., Hu, G., Hart, P. J. & McAlister-Henn, L. Allosteric motions in structures of yeast NAD<sup>+</sup>-specific isocitrate dehydrogenase. *J Biol Chem* **283**, 10872–10880 (2008).
27. Dang, L. *et al.* Cancer-associated IDH1 mutations produce 2-hydroxyglutarate. *Nature* **462**, 739–744 (2009).
28. Zhao, S. *et al.* Glioma-derived mutations in IDH1 dominantly inhibit IDH1 catalytic activity and induce HIF-1 $\alpha$ . *Science* **324** (2009).
29. Yang, B., Zhong, C., Peng, Y., Lai, Z. & Ding, J. Molecular mechanisms of “off-on switch” of activities of human IDH1 by tumor-associated mutation R132H. *Cell Res* **20**, 1188–1200 (2010).
30. Laurenti, G. & Tennant, D. A. Isocitrate dehydrogenase (IDH), succinate dehydrogenase (SDH), fumarate hydratase (FH): three players for one phenotype in cancer? *Biochem Soc Trans* **44**, 1111–1116 (2016).
31. Dang, L., Yen, K. & Attar, E. C. IDH mutations in cancer and progress toward development of targeted therapeutics. *Ann Oncol* **27**, 599–608 (2016).
32. Waitkus, M. S., Diplas, B. H. & Yan, H. Isocitrate dehydrogenase mutations in gliomas. *Neuro Oncol* **18**, 16–26 (2016).
33. Hartong, D. T. *et al.* Insights from retinitis pigmentosa into the roles of isocitrate dehydrogenases in the Krebs cycle. *Nat Genet* **40**, 1230–1234 (2008).
34. Zeng, L. *et al.* Aberrant IDH3 $\alpha$  expression promotes malignant tumor growth by inducing HIF-1-mediated metabolic reprogramming and angiogenesis. *Oncogene* **34**, 4758–4766 (2015).
35. Yoshimi, N. *et al.* Cerebrospinal fluid metabolomics identifies a key role of isocitrate dehydrogenase in bipolar disorder: evidence in support of mitochondrial dysfunction hypothesis. *Mol Psychiatry*, 10.1038/mp.2015.217 (2016).
36. Yamada, S. *et al.* NAD-dependent isocitrate dehydrogenase as a novel target of tributyltin in human embryonic carcinoma cells. *Sci Rep* **4**, 5952 (2014).
37. Ramachandran, N. & Colman, R. F. Evidence for the presence of two nonidentical subunits in NAD-dependent isocitrate dehydrogenase of pig heart. *Proc Natl Acad Sci USA* **75**, 252–255 (1978).
38. Huang, Y. C., Bailey, J. M. & Colman, R. F. Inactivation of NAD-dependent isocitrate dehydrogenase by affinity labeling of the allosteric ADP site by 2-(4-bromo-2,3-dioxobutylthio)adenosine 5'-diphosphate. *J Biol Chem* **261**, 14100–14107 (1986).
39. Ma, T., Peng, Y., Huang, W. & Ding, J. Molecular mechanism of the allosteric regulation of the  $\alpha\gamma$  heterodimer of human NAD-dependent isocitrate dehydrogenase. *Sci Rep* **7**, 40921 (2017).
40. Dyrlov Bendtsen, J., Nielsen, H., von Heijne, G. & Brunak, S. Improved prediction of signal peptides: SignalP 3.0. *J Mol Biol* **340**, 783–795 (2004).
41. Scheich, C., Kümmel, D., Soumailakakis, D., Heinemann, U. & Büsow, K. Vectors for co-expression of an unrestricted number of proteins. *Nucleic Acids Res* **35**, e43 (2007).
42. Foltá-Stogniew, E. Oligomeric states of proteins determined by size-exclusion chromatography coupled with light scattering, absorbance, and refractive index detectors. *Methods Mol Biol* **328**, 97–112 (2006).

## Acknowledgements

This work was supported by grants from the National Natural Science Foundation of China (31170690 and 31521061), the Ministry of Science and Technology of China (2013CB910404) and the Chinese Academy of Sciences (XDB08010302). We thank other members of our group for technical assistance and helpful discussion.

## Author Contributions

T.M. carried out the cloning, protein purification and biochemical studies. Y.P. and W.H. participated in the initial cloning, expression and purification experiments. Y.L. participated in the biochemical studies. J.D. conceived the study, participated in the designs and data analyses of all experiments, and wrote the manuscript.

## Additional Information

**Supplementary information** accompanies this paper at <http://www.nature.com/srep>

**Competing financial interests:** The authors declare no competing financial interests.

**How to cite this article:** Ma, T. *et al.* The  $\beta$  and  $\gamma$  subunits play distinct functional roles in the  $\alpha_2\beta\gamma$  heterotetramer of human NAD-dependent isocitrate dehydrogenase. *Sci. Rep.* 7, 41882; doi: 10.1038/srep41882 (2017).

**Publisher's note:** Springer Nature remains neutral with regard to jurisdictional claims in published maps and institutional affiliations.



This work is licensed under a Creative Commons Attribution 4.0 International License. The images or other third party material in this article are included in the article's Creative Commons license, unless indicated otherwise in the credit line; if the material is not included under the Creative Commons license, users will need to obtain permission from the license holder to reproduce the material. To view a copy of this license, visit <http://creativecommons.org/licenses/by/4.0/>

© The Author(s) 2017